≪Research Paper≫ Applied Science and Convergence Technology Vol.24 No.4, July 2015, pp.102~110
http://dx.doi.org/10.5757/ASCT.2015.24.4.102

Numerical Modeling of Floating Electrodes in a Plasma Processing System

Junghoon Joo*

Graduate Program of Plasma Convergence Engineering & Plasma Materials Research Center, Kunsan National University, Gunsan 573-701, Korea

(Received July 29, 2015, Accepted July 30, 2015)

Fluid model based numerical analysis is done to simulate a plasma processing system with electrodes at floating potential. V_f is a function of electron temperature, electron mass and ion mass. Commercial plasma fluid simulation softwares do not provide options for floating electrode boundary value condition. We developed a user subroutine in CFD−ACE+ and compared four different cases: grounded, dielectric, zero normal electric field and floating electric potential for a 2D−CCP (capacitively coupled plasma) with a ring electrode.

Keywords : Numerical modeling, Capacitively coupled plasma, Floating potential, CFD−ACE+

I. Introduction

Plasma simulations by using a fluid model is useful in designing low temperature plasma processing systems: dry etcher, PECVD, plasma asher, ion doping systems [1−4]. Numerical model can be setup either by PIC (particle−in−cell) or by fluid model. Computer hardware performance limits the usability of PIC in rather simple geometry with inert gas chemistries. Plasma etch/deposition uniformity over a large size substrate (e.g. 8th generation glass system in LCD industry) has been improved by many ideas. Using electrodes with floating electric potential could be a way to control plasma uniformity. Dielectric surfaces collect charges and reduces sheath electric field. Grounded conductor surfaces are invoking higher electric field than dielectric surfaces. CCP (capacitively coupled plasma) design should have powered electrodes and surrounding dielectric guides. Horizontally diffusing plasma may be controlled by secondary electrodes with dielectric, grounded and floating potential. Commercial plasma fluid modeling software packages didn't supply floating potential boundary condition option [5]. By developing a user subroutine in ESI's CFD−ACE+ package, floating electrode option was available and compared with three other boundary conditions: grounded, dielectric and surface charge density.

II. Numerical Model Setup

Plasma fluid equations are valid in moderate gas pressure (higher than mTorr). Inductively coupled plasmas (ICP) and CCP are well represented by this fluid model. CFD−ACE+ is a commercial fluid code either by Maxwellian electron energy distribution or by direct solving Boltzmann equation [6]. In most

* [E−mail] jhjoo@kunsan.ac.kr

cases with complex chemical reactions, all of the necessary electron collision cross section data may not be available. Maxwellian distribution assumption becomes the second choice. It would not make great difference in common applications of low temperature processing plasmas [7].

Floating potential surfaces can be classified into three categories in Fig. 1. Oxide on a conductor is the most common case in plasma processing systems to protect the surface from reactive gases as in Fig. 1(c). Plasma fluid model has B.C. (boundary condition) setting step for variables. For electron temperature, one can choose from three options: fixed T_e, gradient and thermal flux balance. CFD-ACE+ is using FVM (finite volume method) which is popular in fluid dynamic simulation scheme. TFB (thermal flux balance) B.C. is letting the electron energy to be delivered toward the boundary [8]. Formulation is as following in Eqn. 1~3.

$$\frac{3}{2}\frac{\partial}{\partial t}(n_e T_e)+\nabla\left(\frac{5}{2}T_e\overrightarrow{\Gamma_e}-\chi\nabla T_e\right)=P-n_e\sum_r n_r k_r \varepsilon_r \quad (1)$$

$$\chi=\frac{5}{2}n_e D_e \quad (2)$$

$$\overrightarrow{\Gamma_e}=\mu_e n_e\nabla\phi-D_e\nabla n_e \quad (3)$$

P: power absorption
μ_e: the electron mobility
D_e: the diffusion coefficient
ϕ: the electrostatic potential
T_e: the electron temperature
n_e: the electron density
k_r: the rate constant for r-th reaction
ϵ_r: energy consumption of r-th reaction
Γ_e: electron flux

A user subroutine coded in Fortran90 is developed to build floating potential B.C. setting in CFD-ACE+ as the source code partially shown in Fig. 2. User can communicate to solver via user variables in CFD-ACE-GUI menu. Floating potential can be obtained by the equation (4)~(5).

$$V_f=\frac{kT_e}{2e}ln\left(\frac{m_i}{2\pi m_e}\right)=\frac{kT_e}{e}\left(2.8+\frac{1}{2}ln\mu_i\right) \quad (4)$$

$$\mu_i=\frac{m_i}{m_e} \quad (5)$$

V_f: the floating potential
T_e: the electron temperature
m_i: the mass of ion
m_e: the mass of electron

Determining of the floating potential is reduced to finding electron temperature values and ion mass. In a single ion species plasma, it is direct to get, but in complex ion plasmas (in most of processing plasma environments), m_i can be obtained via ion flux weighting. For an example, H_2^+ gives V_f=6.9 T_e and Ar^+ gives 8.38 T_e. Assuming the electron temperature in the range of 1 to 10 eV, the floating potential will

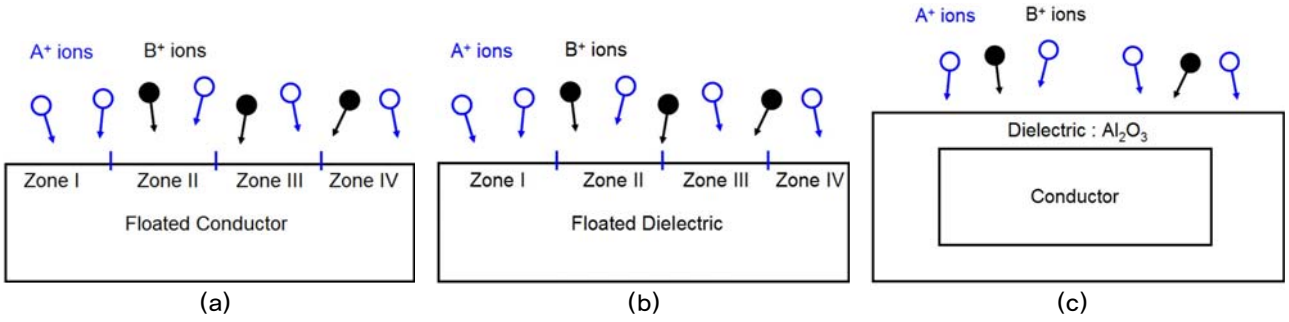

Figure 1. Electrically floating electrode surfaces (a) conductor, (b) dielectric, (c) dielectric on conductor.

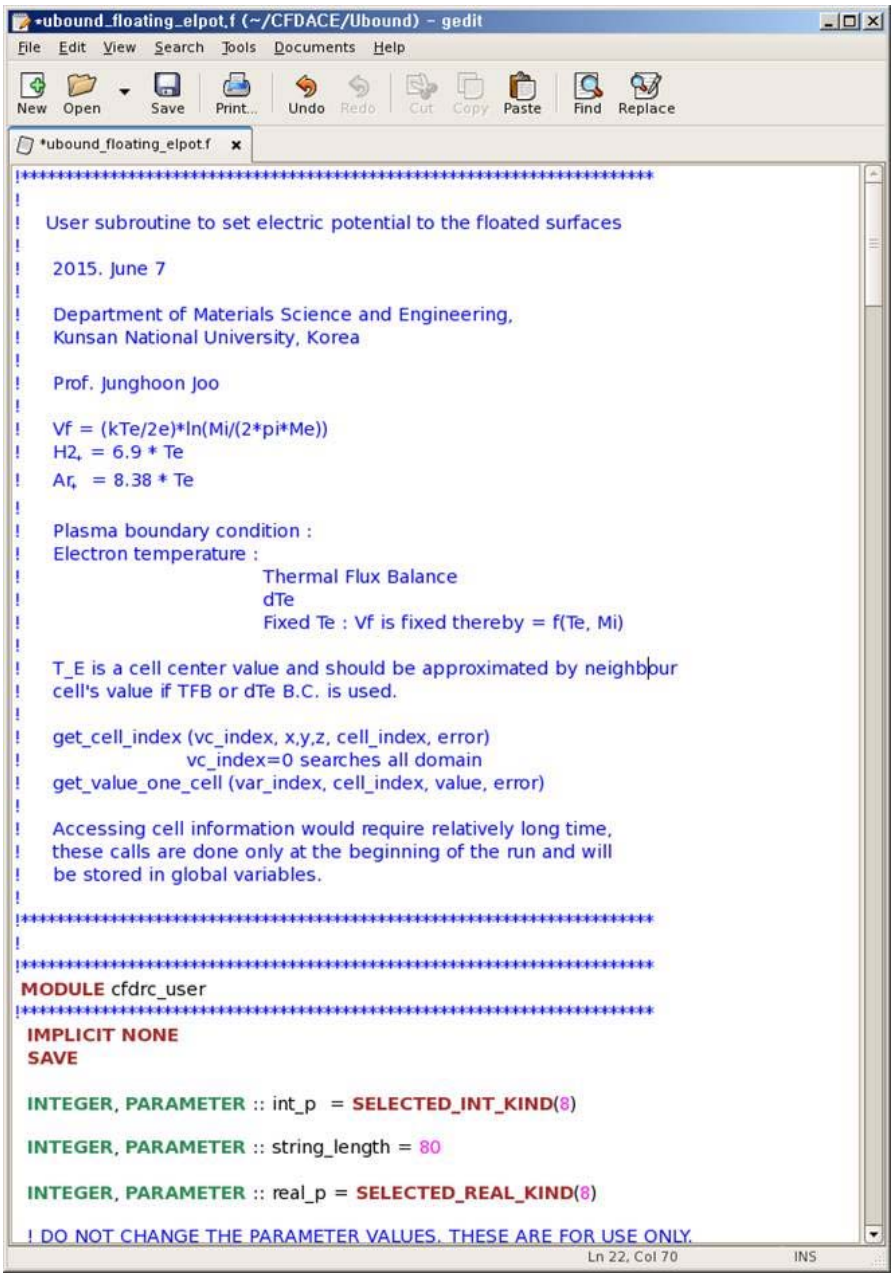

Figure 2. User subroutine coded in Fortran90 to build floating potential B.C.

be between 6.9 V and 83.8 V in accordance with rf period. It will be staying in positive values only. Dielectric surfaces often collect charges and have a limited conductivity to leak some of them. This feature is also realized in CFD-ACE+ as called in lossy dielectric with limited electrical conductivity option. Surface charge state is not easy to simulate in a numerical model. The secondary electron emission coefficient is well constant over ion's kinetic energies range of 100~1000 eV [9] for many gases. Light ions, e.g. He^+ has 0.24, and Ar^+ has 0.1. Heavy ions, e.g. Xe^+ shows very low value of 0.02 which is 1/5 of Ar^+ and 1/10 of He^+. For an example, a mixed gas environment to deposit silicon nitride, H_2+He+N_2+SiH_4 mixture is often used and each ions will have much different the ionic secondary emission coefficient on the electrode surfaces. In the test case running of Ar CCP, a constant value of 0.1 is used as an ionic

secondary emission coefficient.

For electron flux calculation on the surfaces, equation (6)～(11) are used.

$$\Gamma_{e,n} = \frac{1}{4} n_e v_{e,th} - \gamma \sum_i (q_i \Gamma_{i,n}) \quad (6)$$

$$v_{e,th} = (\frac{8 k_B T_e}{\pi m_e})^{1/2} \quad (7)$$

$v_{e,th}$: the electron thermal velocity

γ: the secondary emission coefficient

q_i: ion species charge

$\Gamma_{i,n}$: ion number flux

$$\frac{5}{2} T_e \Gamma_{e,n} - \chi \frac{\partial T_e}{\partial n} = 2 T_e (\frac{1}{4} n_e v_{e,th} - \gamma \sum_i q_i \Gamma_{i,n}) \quad (8)$$

$$-\nabla \cdot \epsilon \nabla \phi = e(\sum_i q_i n_i - n_e) \quad (9)$$

$$\frac{\partial \sigma}{\partial t} = e[\sum_i q_i \Gamma_{i,n} - \Gamma_{e,n}] \quad (10)$$

$$\epsilon E_n - \epsilon_2 E_{2n} = -\sigma_s \quad (11)$$

$E_n = -\partial\phi/\partial n$: normal component of the field on the surface

n: pointing from the plasma to the dielectric regions

Fig. 3(a) and 3(b) show the geometrical model for test simulation of the above floating potential model. 2D axi-symmetric model for a diameter 360 mm and an electrode gap of 60 mm. RF power electrode (diameter 280 mm) is used as a gas inlet plate as well. A floated ring of 20 mm rectangular cross section and average diameter of 300 mm is inserted at z=30 mm. A dual time step scheme is used. The shared time step of 10^{-6} sec is used for flow dynamics calculation and 1/40 of rf period is used for all plasma related equations. This ring is a virtual setting for the confirmation of the user subroutine.

III. Simulation Results and Discussion

1. Gas flow characteristics

Velocity magnitude and vector presentation are

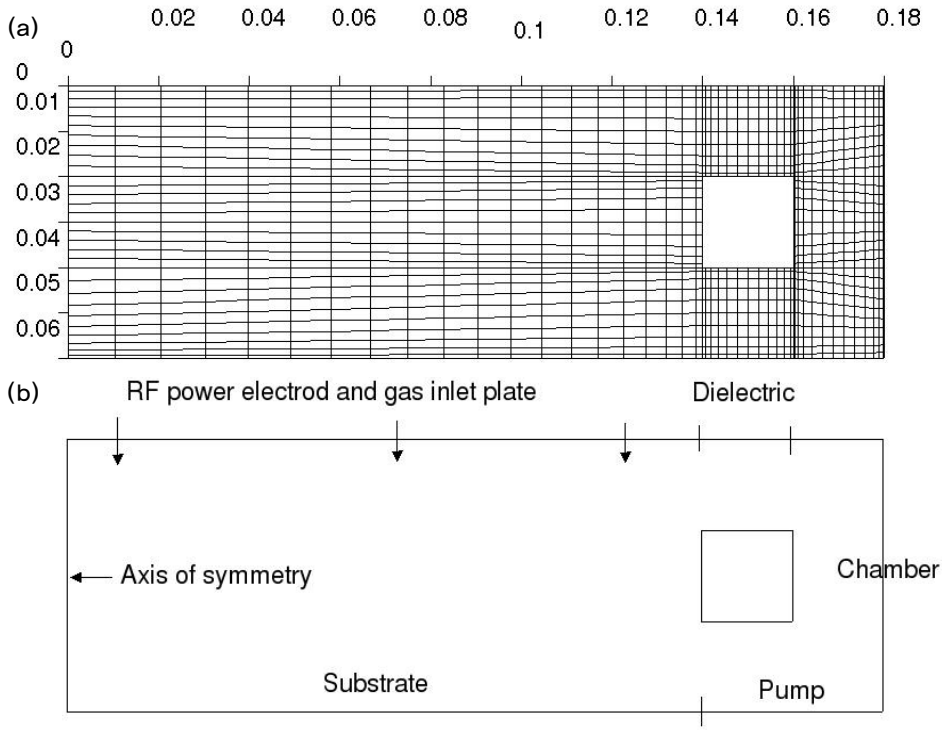

Figure 3. Geometrical model for test case simulation of the floating potential user subroutine.

shown in Fig. 4. Floated ring is a virtual object designed in this study. In real world, it should be supported by a dielectric material attached to the chamber. Uniform gas inlet velocity of 0.2 m/s was assumed at chamber pressure of 400 mTorr. Fluid model is effective in this pressure range. Gas velocity at 5 mm above the substrate was varying from nearly 0 m/s (center) to 0.3 m/s (edge). From r=0.1 m, the gas flow started to be accelerated. Gas flow velocity around the ring showed faster values at the region below the ring. It would affect the neutral density and related electron chemical reactions, e.g. two step ionization of Ar metastable. In case of complicated molecules, dissociated radicals would be controlled by gas flow profile as well as electric field distribution.

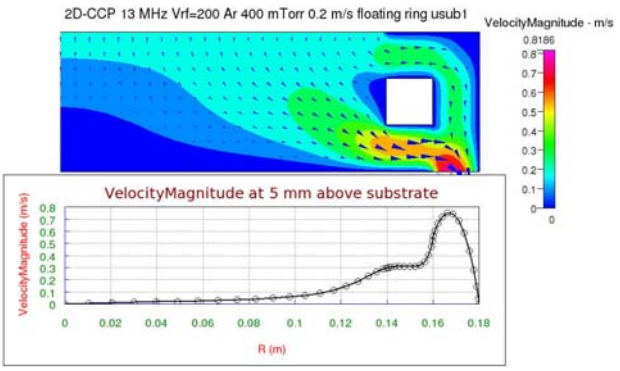

Figure 4. Gas flow dynamic simulation result.

2. RF power absorption profile

This model uses Ohmic heating as a power

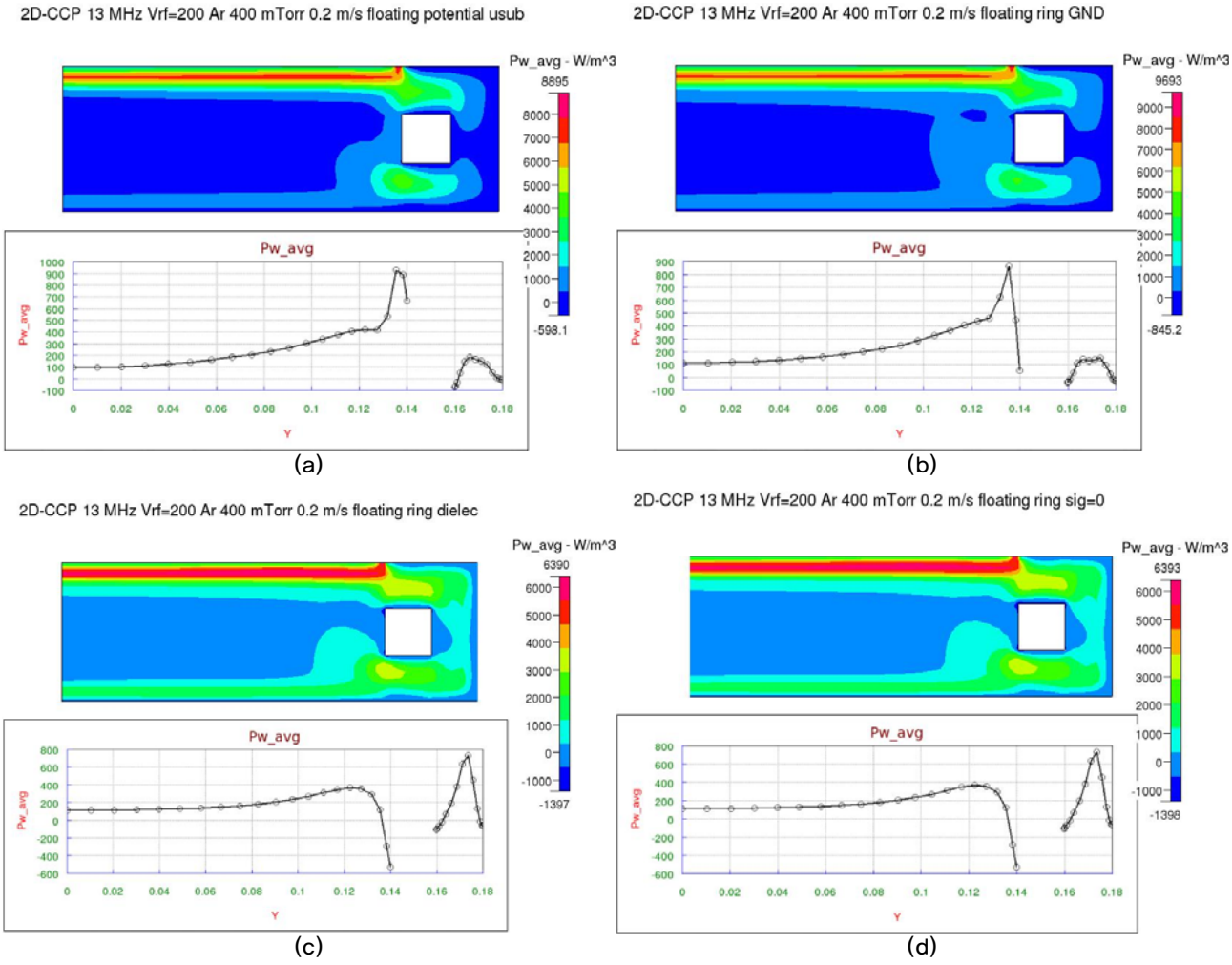

Figure 5. Time averaged power absorption profile for (a) floated (b) grounded (c) dielectric (d) sig=0.

absorption scheme. Fig. 5(a)～5(d) show the effects of surface potential B.C. This simulation was done with a same rf voltage condition on the powered electrode. Four each model showed slightly different total absorbed power. Through these models, relative comparison of power absorption profiles are used to check the effects of the ring's surface B.C. Power absorption around the ring for floating and grounded models are showing similar results. Right side region of the ring has virtually no power absorption. Dielectric and zero surface charge density models showed higher power absorption in the right side region of the ring than the two models. Resistive power absorption is calculated by $\vec{J} \cdot \vec{E}$. Higher charged species current density or electric field is a condition for higher power absorption. Floated potential case showed highest power absorption in left side of the ring which is close to the rf powered electrode. Attached line graphs are drawn at the mid plane z=30 mm.

3. Electron temperature profile

RF period averaged electron temperature profile for four different models are shown in Fig. 6. Similar to power absorption profiles, electron temperature showed a steep profile in left side of the ring, but relatively uniform profile in the discharge region than other cases. For dielectric and sig=0 cases, chamber corners showed localized high electron temperature profile. It may play a weak point in reactive processing chemistries.

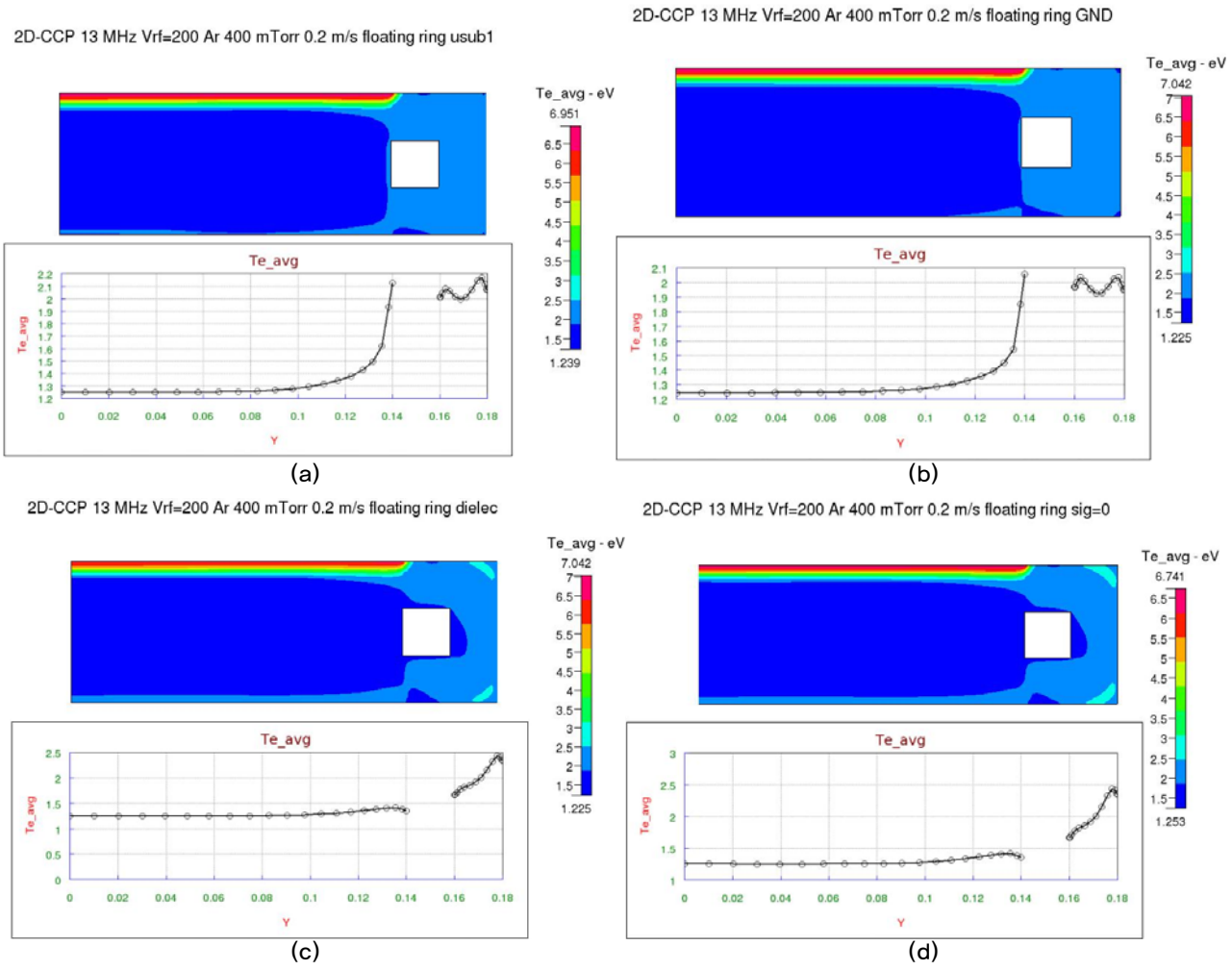

Figure 6. Time averaged electron temperature profile for (a) floated (b) grounded (c) dielectric (d) sig=0.

There are many electron collision reactions occurring around 1∼2 eV of Maxwellian average temperature.

As in Eqn. (4), the floating potential is a function of ion mass and electron temperature. As, the B.C. for T_e is directly determining the floating potential, the nearest cell's T_e is substituted instead. Otherwise, the floating potential model would not make any difference but assigning a calculated electric potential value somewhere between 0 and 10 V depending on the B.C. for T_e.

4. Electric potential profile

The most drastic difference among four models is in electric potential profile as expected. Fig. 7 is showing the electric potential profile at rf phase 0. The line graph along the center line (z=30 mm) in floating electrode case symmetric result around 7 V. Dielectric case and sig=0 case showed higher surface potential around 25 V with less stiff sheath potential gradient. The surface potential is varying in accordance with rf sine wave. Other models, grounded, dielectric or sig=0, gave much different fashion in time varying electric potential distribution. Grounded potential model showed the most confined plasma potential profile in Fig. 7(b).

As shown in Fig. 1(c), thin dielectric surface layer would be challenging to numerical simulation. Positive ion recombination requires leakage current from base conductor through the dielectric layer to make charge

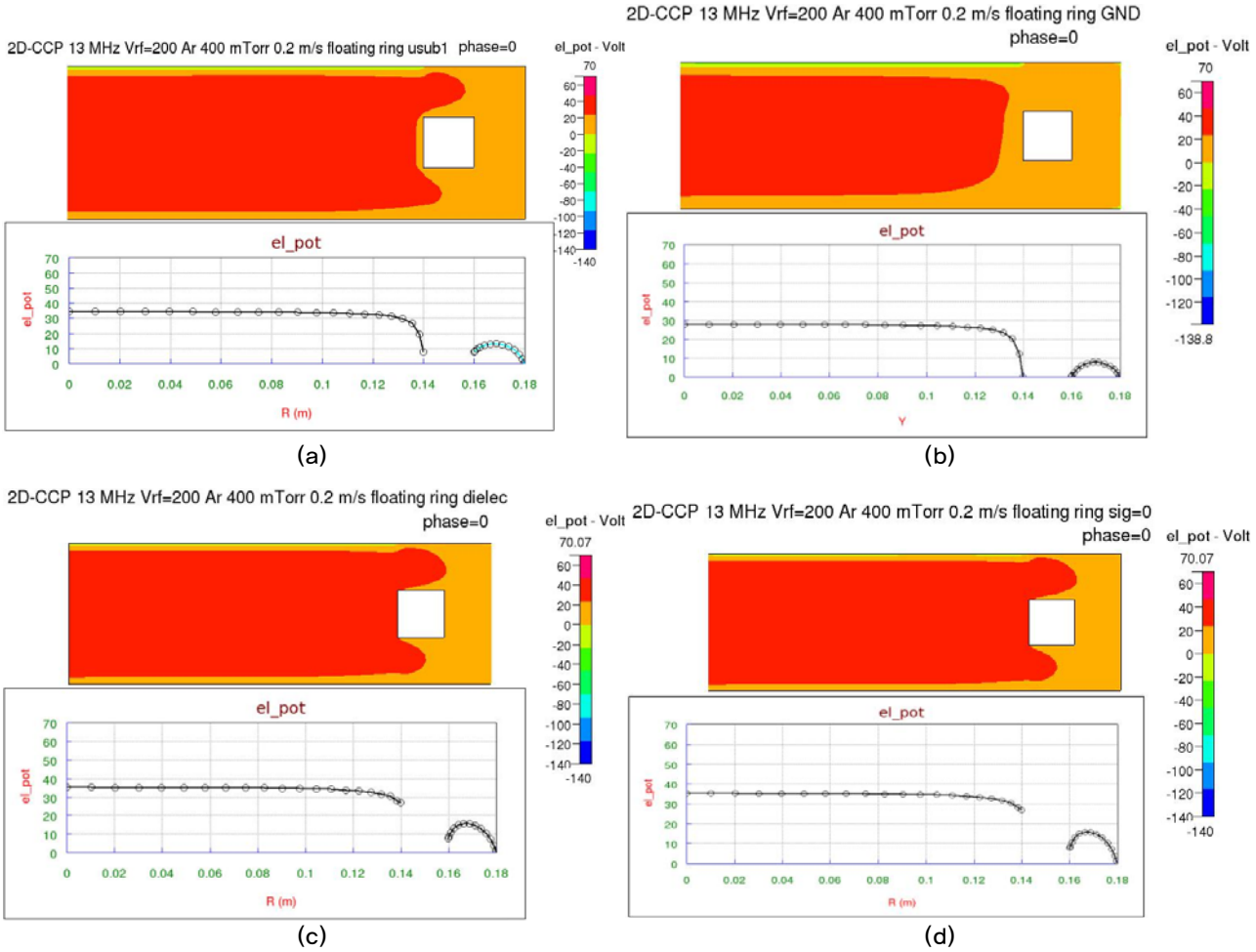

Figure 7. Electric potential profile at phase=0 for (a) floated (b) grounded (c) dielectric (d) sig=0.

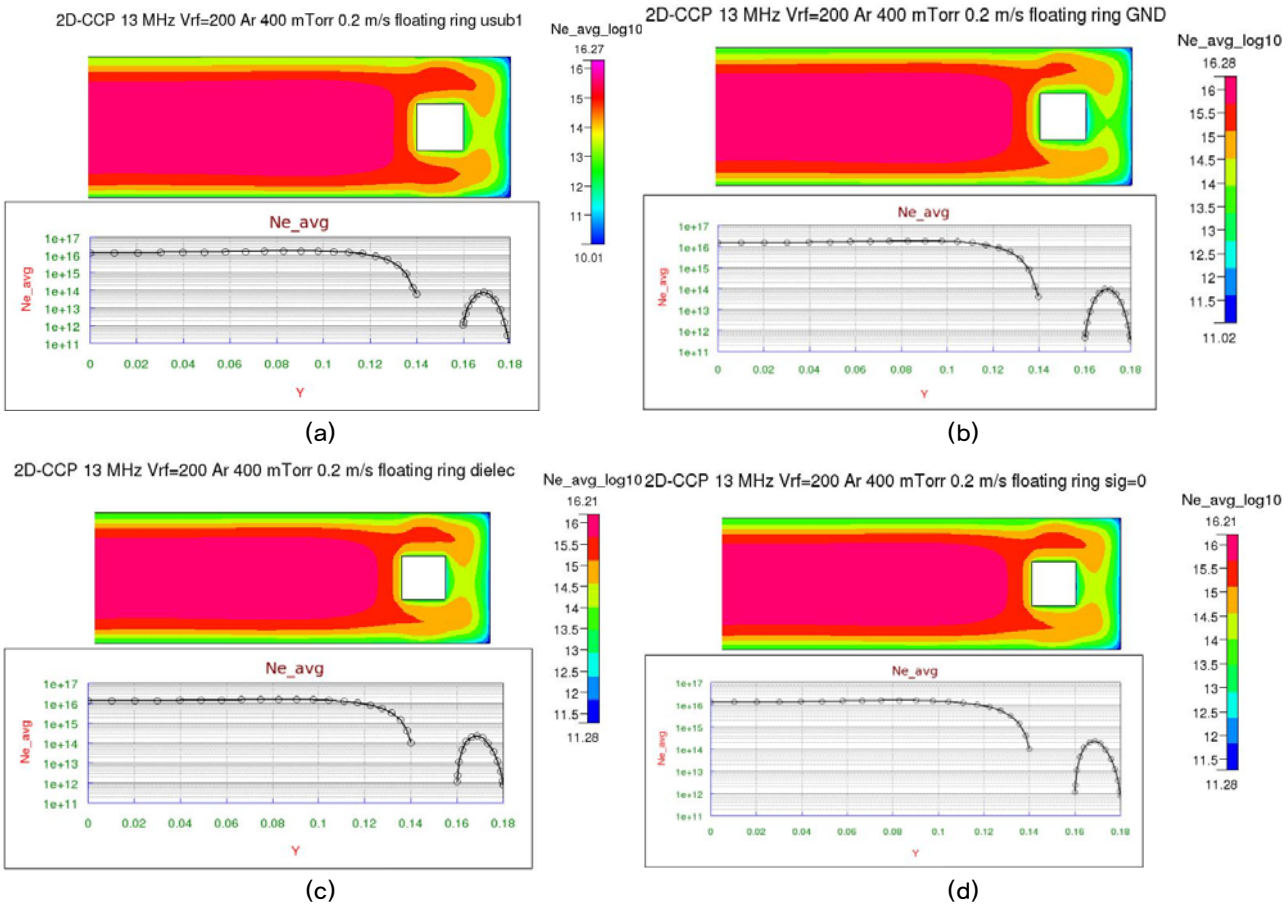

Figure 8. Time averaged electron density profile for (a) floated (b) grounded (c) dielectric (d) sig=0.

balance of the surface. Otherwise, the surface would be gradually charged positive. This topic would be thoroughly addressed in other report together with incoming ion flux changes.

5. Electron density profile

The least changed plasma property of these models seems to be electron density at a glance. Floating potential case showed the most uniform profile around the ring. Fig. 8 shows electron density profile in log scale. Line graphs are drawn along the center line. Ground potential model showed the lowest electron density in left side of the ring. The right and lower side region of the ring showed difference in surface electric potential boundary conditions. Floating potential model (Fig. 8(a)) showed most overpassing feature of the electrons around the ring. In contrast, grounded potential model showed most plasma blocking fashion. Electron density profile is affected strongly by ion transport as well as ion pair creation. Under 400 mTorr of relatively high gas pressure, frequent collision would limit ion's diffusion and drift. Pressure variation and other investigation of the process variables will be addressed in other reports.

IV. Conclusions

A user subroutine to assign electrically floating potential boundary condition to a commercial multi physics based plasma fluid simulation tool, CFD-ACE+, is developed and applied to a 2D-CCP of Ar 400 mTorr. For comparison, electrically grounded, dielectric

and zero surface charge density models are used. Rf power absorption, electric potential, electron temperature and density profiles are compared and showed much different fashion especially in electric potential. In rf power absorption, dielectric ring gave more uniform profile than floated or grounded ring. Electron density distribution showed the least change in four models.

Acknowledgements

This work was supported by the Industrial Strategic technology development program (10041926, Development of high density plasma technologies for thin film deposition of nanoscale semiconductor and flexible display processing) funded by the Ministry of Knowledge Economy (MKE, Korea).

References

[1] D.C. Kwon, N.S. Yoon, J.H. Han and J.W. Shon, Cur. Appl. Phys. **9**, 546 (2009).
[2] J. Joo, J. Kor. Inst. Surf. Eng. **43**, 154 (2010).
[3] J. Joo, J. Kor. Vac. Soc. **19**, 331 (2010).
[4] J. Joo, J. Kor. Inst. Surf. Eng. **45**, 174 (2012).
[5] B. Briehl, H. Urbassek, Surf. Coat. Technol. **160**, 259 (2002).
[6] V. Kolobov, R. Arslanbekov, Microelec. Eng. **69**, 606 (2003).
[7] D. Economu, Thin Solid Films **365**, 348 (2000).
[8] CFD-ACE+ module manual II, 2014.
[9] H. D. Hagstrum, Phys. Rev. **104**, 672 (1956).